Origin and serpentinization of ultramafic rocks in dismembered ophiolite north of Trembleur Lake, central British Columbia

Katrin Steinthorsdottir[1, a], Jamie Cutts[1], Greg Dipple[1], Dejan Milidragovic[2], and Frances Jones[1]

[1] Bradshaw Research Initiative for Minerals and Mining, Department of Earth, Ocean and Atmospheric Sciences, University of British Columbia, Vancouver, BC, V6T 1Z4
[2] British Columbia Geological Survey, Ministry of Energy, Mines and Petroleum Resources, Victoria, BC, V8W 9N3
[a] corresponding author: ksteinth@eoas.ubc.ca

Abstract

Serpentinization of ultramafic rocks can produce alteration minerals such as brucite ($Mg(OH)_2$), which has the potential to sequester carbon dioxide, and awaruite (Ni_3Fe), a potential source of nickel. The Trembleur ultramafite is part of a dismembered ophiolite in central British Columbia. Field and petrographic data indicate that it is heterogeneous both in protolith and alteration. The protolith consists mainly of harzburgite, lherzolite, dunite, and lesser pyroxenite. Dunite, more abundant than previously recognized, could be a replacement of harzburgite (±lherzolite). All ultramafic rocks in the Decar area, north of Trembleur Lake, are altered to some extent (mainly partially to pervasively serpentinized) and locally contain higher temperature metamorphic assemblages. Carbonate alteration post-dated serpentinization, degrading minerals such as brucite and awaruite to locally produce ophicarbonates, soapstone, and listwanite. The primary olivine-pyroxene ratio of the protolith may have controlled fluid pathways and thus the extent of serpentinization and the abundance, distribution, and grain size of brucite and awaruite, which has implications for carbon sequestration and nickel potential in the Decar area.

Keywords: Trembleur ultramafite, Decar, Baptiste deposit, serpentinite, listwanite, CO_2 sequestration, brucite, awaruite, dunite, harzburgite, lherzolite, pyroxenite

1. Introduction

Alteration of ophiolitic rocks is common and includes hydration (e.g., serpentinization) and carbonation (e.g., formation of listwanite). Serpentinization produces minerals such as serpentine, magnetite, brucite ($Mg(OH)_2$), and awaruite (Ni_3Fe; O'Hanley, 1996). Brucite, along with serpentine, can react with and sequester atmospheric CO_2 in carbonate minerals (Power et al., 2013) and awaruite forms with serpentinization in reducing environments from primary olivine or sulphides and is a potential source of nickel (Eckstrand, 1975; Britten, 2017). Listwanite is formed by the dehydration and carbonate alteration of these hydrated minerals and is a natural analogue of CO_2 sequestration through mineral carbonation (Hansen et al., 2005). Characterizing the chemical, mineralogical, and textural variability of a protolith is key to constraining its variable alteration to serpentinite and listwanite (Hall and Zhao, 1995; Hansen et al., 2005; Milidragovic and Grundy, 2019).

The Trembleur ultramafite is in the southern segment of the Cache Creek terrane, which extends through British Columbia into southern Yukon (Fig. 1; e.g., Monger and Gibson, 2019). The Trembleur ultramafite in the Decar area form part of a dismembered supra-subduction zone ophiolite and is variably serpentinized and carbonate-altered (Britten, 2017;

Milidragovic and Grundy, 2019). The ultramafic protoliths are heterogeneous and consists of diverse peridotites and lesser pyroxenites. The serpentinized ultramafic rocks in the Decar area contain brucite, of potential environmental value (e.g., Vanderzee et al., 2019) and awaruite (Ni_3Fe), of potential economic value (Britten, 2017). This contribution summarizes the field and petrographic results of a study designed to evaluate the protoliths and alteration of the Trembleur ultramafite in order to constrain the controls on the formation, distribution, and abundance of brucite and awaruite and to identify the extent of alteration in the field.

2. Geological setting

The Decar area is underlain by rocks of the Cache Creek terrane, a tectonostratigraphic unit that contains Late Devonian to Middle Jurassic oceanic rocks and extends from southern British Columbia to Yukon (Fig. 1a; Cordey et al., 1991; Golding et al., 2016). These oceanic rocks were deformed and metamorphosed by ca. 172 Ma, following collision with the Stikine terrane on its western flank (Mihalynuk et al., 1994; Struik et al., 2001; Mihalynuk et al., 2004; Monger and Gibson, 2019). Exposed in the area are: greenschist- to amphibolite-facies ultramafic to intermediate igneous rocks

49

Geological Fieldwork 2019, British Columbia Ministry of Energy, Mines and Petroleum Resources, British Columbia Geological Survey Paper 2020-01
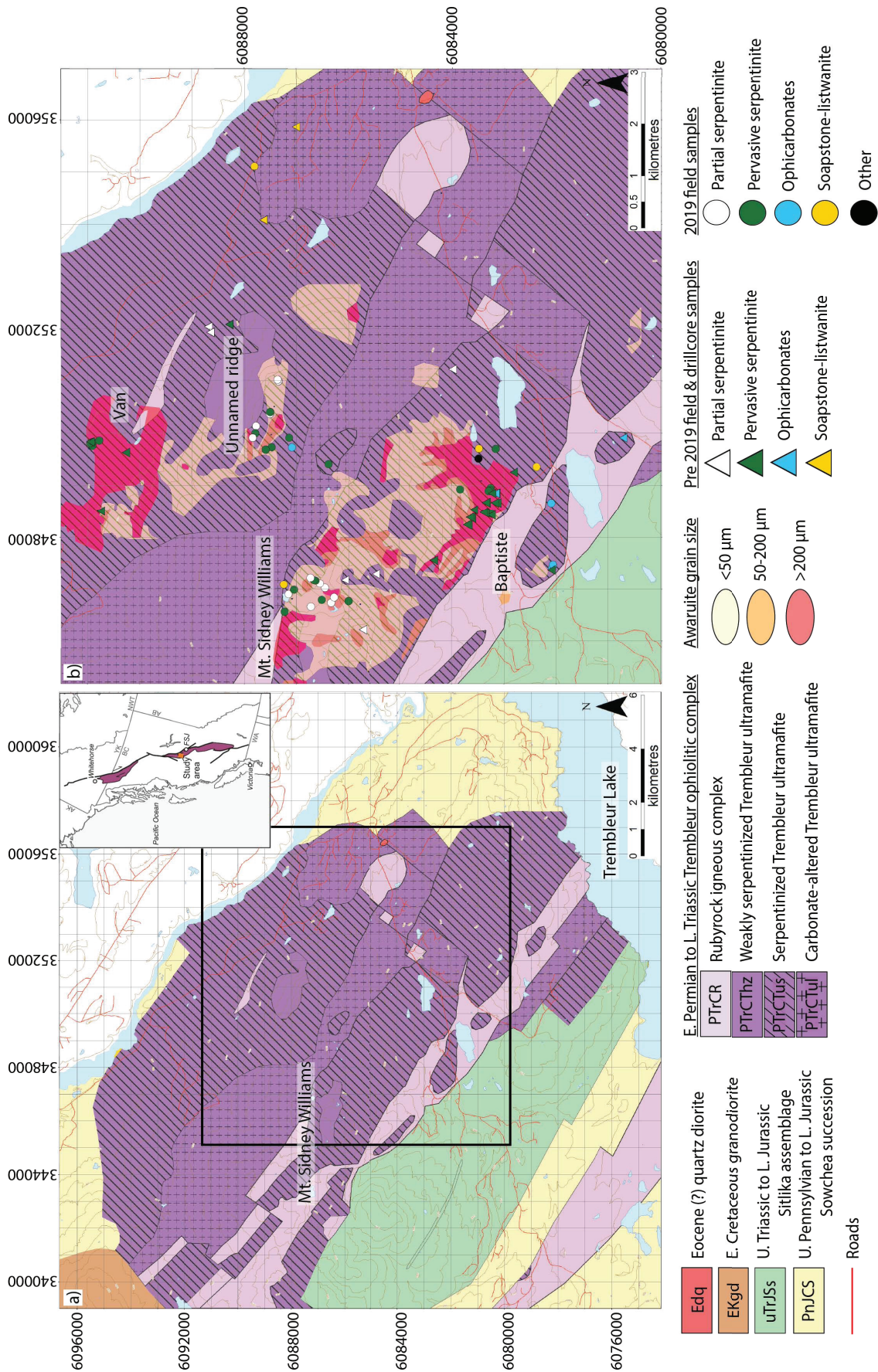
Fig. 1 **a)** Geological map of the area north of Trembleur Lake. **b)** Geological map of the Decar area with sample locations and mapped awaruite grain size. Modified from Britten (2017) and Milidragovic (2019).

and metasedimentary rocks of the Rubyrock igneous complex (early Permian to Late Triassic); altered ultramafic rocks of the Trembleur ultramafite (early Permian to Late Triassic); volcanic, siliciclastic, and carbonate rocks of the Sowchea succession (Upper Pennsylvanian to Lower Jurassic); and sedimentary and volcanic rocks of the Sitlika assemblage (Upper Triassic to Lower Jurassic; Fig. 1a; for details see Milidragovic et al., 2018; Milidragovic, 2019). The rocks are exposed in fault-bounded, northwest-trending belts that are dismembered by cross faults. The Sowchea succession and parts of the Sitlika assemblage are interpreted to record volcanism and sedimentation in an intraplate oceanic setting (Schiarizza and Massey, 2010; Milidragovic and Grundy, 2019). In contrast, the Rubyrock igneous complex and Trembleur ultramafite are interpreted to represent the crustal and mantle sections of a dismembered supra-subduction zone ophiolite (Schiarizza and MacIntyre, 1999; Struik et al., 2001; Schiarizza and Massey, 2010; Britten 2017; Milidragovic and Grundy, 2019). In this contribution, we focus on the Trembleur ultramafite.

The least serpentinized and carbonate-altered rocks of the Trembleur ultramafite outcrop in areas of relatively high elevation on Mount Sidney Williams (also known as Mount Sidney, Tselk'un or Red Rock) and an unnamed ridge ca. 3 km ENE of Mount Sidney Williams (Fig. 1b). In contrast, the most altered rocks occupy areas of low elevation. Highly serpentinized areas host awaruite, which is coarse grained at Baptiste and other places in the area (shown as irregular red polygons in Fig. 1b; Britten, 2017). Variable abundances of brucite have been documented in the highly serpentinized area in the Baptiste area (Vanderzee et al., 2019), but abundances are unknown in other parts of the Trembleur ultramafite. Ophicarbonate (serpentine-magnesite), soapstone (talc-magnesite), and listwanite (magnesite-quartz) assemblages are mainly in the southeastern and eastern part of the Trembleur ultramafite (Milidragovic et al., 2018).

3. Methods

A total of 89 hand samples of ultramafic rocks were selected for this study (Fig. 1b). Of these, 55 are surface samples collected during the 2019 field season, 15 are surface samples collected during the 2017 field season (Milidragovic and Grundy, 2019), and 19 are cores provided by FPX Nickel Corp. from drilling in nine holes at the Baptiste deposit. Hand samples were selected to represent the full range of alteration and textures of the serpentinized or carbonate-altered Trembleur ultramafite, whereas drill core samples were chosen at various depths (12 to 182 m), to include different rock types, bulk compositions, and mineral content based on Vanderzee et al. (2019).

4. Trembleur ultramafite protolith

The ultramafic rocks at Decar have all undergone some degree of serpentinization or carbonate alteration. Harzburgite (olivine and orthopyroxene-rich, <5% clinopyroxene) is the predominant rock type (Grundy, 2018; Milidragovic and Grundy, 2019), with lesser lherzolite (5-15% clinopyroxene),

and dunite (>90% olivine). Relatively unaltered pyroxenite (>60% pyroxene) dikes and veins are a minor component. These rock types are distinguished in the field by the colour and texture of their weathered surfaces. Weathered surfaces of dunitic rocks are typically smooth and dun compared to more pyroxene-rich rocks, which weather rough and darker brown. The ultramafic rocks are not obviously strained, but shear zones and related folds are locally developed (Figs. 2a, b).

4.1. Harzburgite and lherzolite

Pyroxene-bearing peridotite, spanning the compositional spectrum between harzburgite and clinopyroxene-poor lherzolite, are the most common rocks at Decar. It is difficult to differentiate between the two rock types in the field because most are altered to some extent. Harzburgite (±lherzolite) is composed of olivine (≥60%), orthopyroxene (20-40%), and primary spinel. Orthopyroxene-poor harzburgite (ca. 20% pyroxene), which grades into dunite, is less common and occurs in layers or as pods. Orthopyroxene grains range from <0.5 to1.5 cm and are commonly altered to bastite. The colour of bastite varies in hand specimen from dark grey-green to light grey to white, and in thin section from brown to grey with increasing degree of serpentinization (Figs. 3c, d). Milidragovic et al. (2018) described relatively unaltered spinel harzburgite with coarse orthopyroxene, olivine, and rare finer grained clinopyroxene (Fig. 3c).

Lherzolite is distinguished from harzburgite by more abundant (5-13%) clinopyroxene that occurs as <0.5-1 mm-sized subhedral to euhedral prismatic grains (Fig. 3e). Clinopyroxene occurs as individual grains or as aggregates surrounded by orthopyroxene and/or olivine. Some clinopyroxene grains show lamellae of secondary spinel along cleavage planes. In both lherzolite and harzburgite samples, primary spinel grains vary from <0.3 to 2 mm, range from red to black, and typically show a vermicular or irregular habit, although some are equant. Chlorite and serpentine locally form haloes around spinel, thus spinel could be the source of aluminum for chlorite.

4.2. Dunite

Dunite comprises ca. 15% of all ultramafic rocks at Mt. Sidney and on the unnamed ridge to the east, where it is more abundant than was previously noted by Milidragovic and Grundy (2019). The dunite consists mostly of 1-6 mm equigranular olivine (Fig. 3a) and some samples contain rare brown or grey, fine-grained (<4 mm) bastite after orthopyroxene or clinopyroxene. Fine-grained (<1 mm) unaltered orthopyroxene and clinopyroxene grains are locally (<5%) preserved. Dunite typically occurs within harzburgite (±lherzolite) although it also forms massive uniform outcrops >20 m across. The contact between dunite and harzburgite is typically sharp although rare gradational contacts were also observed. Where dunite is hosted in harzburgite (±lherzolite) it forms sets of parallel to randomly oriented veins or dikes (0.5-50 cm wide), lone dikes, irregular- to lenticular-shaped pods or lenses <1 m wide, or as parallel, discontinuous layers 1-50 cm thick (Fig. 2; Fig. 4a).

51

Geological Fieldwork 2019, British Columbia Ministry of Energy, Mines and Petroleum Resources, British Columbia Geological Survey Paper 2020-01
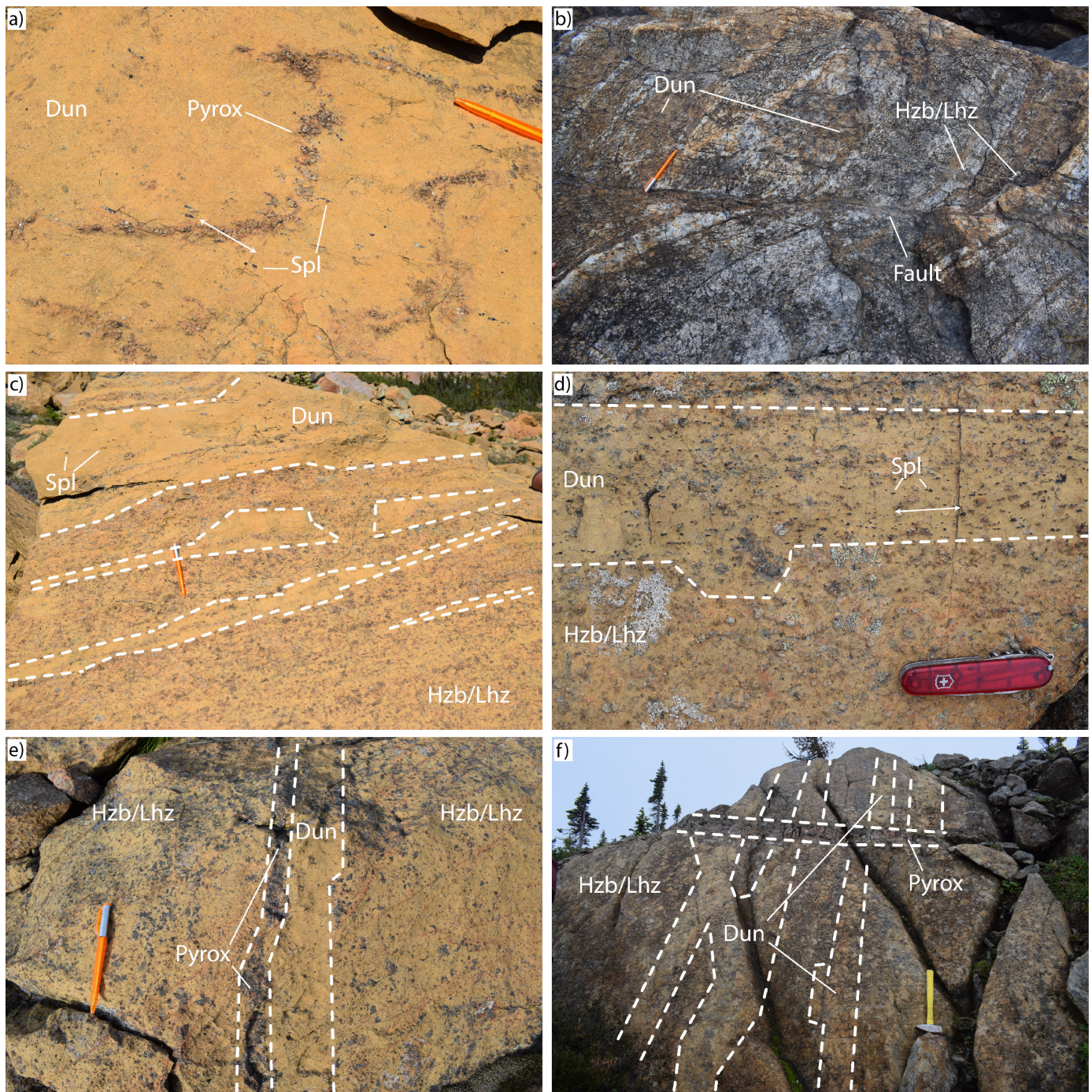
Fig. 2. a) Dunite with thin pyroxenite veins and spinel (Spl) grains. **b)** Centimetre-scale shear zone cutting harzburgite (±lherzolite) and dunite layers. **c)** Dunite with spinel (Spl) as discontinuous layers and irregular pods in harzburgite (±lherzolite). **d)** Coarse spinel (Spl) grains with apparent long axes concordant to the walls of a dunite dike in harzburgite (±lherzolite). **e)** Pyroxenite vein concordant with dunite dike in harzburgite (±lherzolite). **f)** Pyroxenite dike crosscutting dunite and harzburgite (±lherzolite) layers.

Primary spinel is common in dunite and occurs as disseminated grains or multi-crystal aggregates. In plane-polarized light, spinel grains are red to black. Disseminated spinel grains range from <0.5 mm to 0.5 cm and characteristically have an equant habit (Fig. 3a). Apparent long axes of coarse disseminated spinel grains are typically aligned with the walls of the host dunite dikes. Spinel aggregates, which form 0.5-5 cm wide veins, are also aligned with host dunite dikes or layers (Fig. 2d).

Less commonly, thin spinel veinlets are at an angle to dunite dikes and pyroxenite veins and pinch out in peridotite host rock (Fig. 2a).

4.3. Pyroxenite

Pyroxenite typically forms 0.5-5 cm wide veins in dunite layers (Figs. 2a, e) and ca. 10 cm-wide dikes that crosscut dunite and harzburgite (Fig. 2f). The modal abundance

52

Geological Fieldwork 2019, British Columbia Ministry of Energy, Mines and Petroleum Resources, British Columbia Geological Survey Paper 2020-01
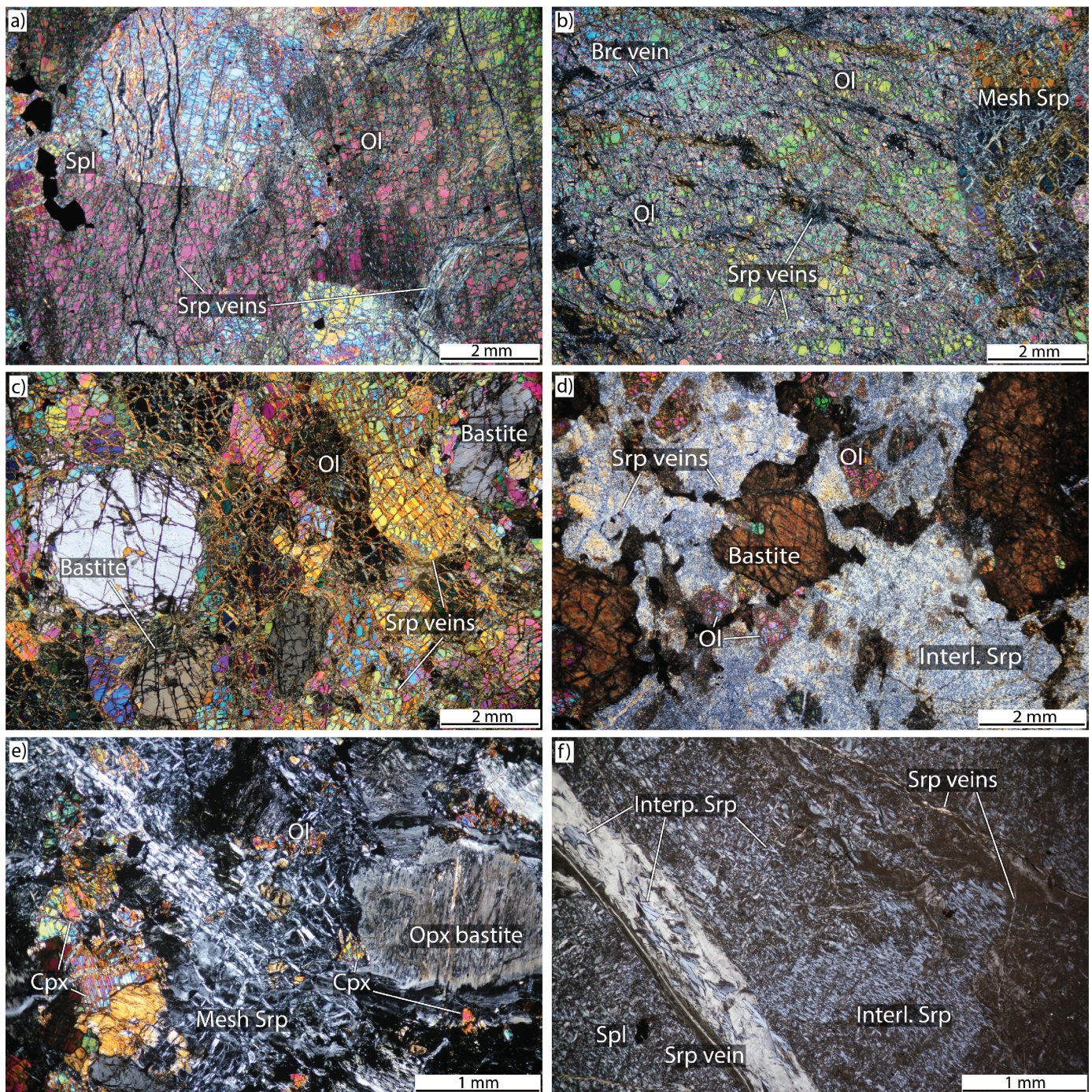
Fig. 3. Partial and pervasive serpentinites. **a)** Partially serpentinized dunite with olivine (Ol), serpentine (Srp) veins and primary spinel (Spl). **b)** Pervasively serpentinized dunite with olivine (Ol), serpentine (Srp) veins, mesh serpentine texture (Mesh Srp), and brucite (Brc) ±serpentine vein. **c)** Partially serpentinized harzburgite (±lherzolite) with bastite grains, olivine (Ol) and serpentine (Srp) veins. **d)** Pervasively serpentinized harzburgite with bastite, relict olivine (Ol), interlocking serpentine texture (Interl. Srp.) and serpentine (Srp) veins. **e)** Pervasively serpentinized lherzolite with clinopyroxene (Cpx), orthopyroxene (Opx) bastite, relict olivine, and mesh serpentine texture (Mesh Srp). **f)** Pervasive serpentinite with a coarse serpentine vein and interlocking serpentine texture (Interl. Srp.) overprinted by interpenetrating serpentine (Interp. Srp.) texture and secondary spinel (Spl). All images are in cross-polarized light.

of orthopyroxene and clinopyroxene in the pyroxenites is variable. In orthopyroxene-rich pyroxenite, the orthopyroxene grains are 4-6 mm with finer grained clinopyroxene, olivine, and red to black spinel of holly leaf texture. In clinopyroxene-rich pyroxenite, the clinopyroxene grains are >2 mm with finer olivine grains.

53

Geological Fieldwork 2019, British Columbia Ministry of Energy, Mines and Petroleum Resources, British Columbia Geological Survey Paper 2020-01

Fig. 4. Partial and pervasive serpentinites, slightly carbonated serpentinites, and listwanite. **a)** Dunite dike in harzburgite (±lherzolite) with serpentine (Srp) veins. **b)** Pervasive serpentinite (Srp) lens in a scaly serpentinite (Srp) matrix. **c)** Pervasive serpentinite with polygonal pattern of serpentine (Srp) veins. **d)** Slightly carbonated pervasive serpentinite with serpentine (Srp) veins, interlocking serpentine texture (Interl. Srp.), carbonate grains (Cb), and secondary spinel (Spl) (crossed-polarized light). **e)** Nearly fully carbonated serpentinite showing relict serpentinite (Srp) texture. **f)** Listwanite with a quartz (Qtz) vein bounded by fuchsite.

5. Serpentinized Trembleur ultramafite

All the rocks we observed in the field and collected for this study are serpentinized and/or carbonated to some extent. For ease of discussion, we subdivide the altered rocks into partial serpentinite, pervasive serpentinite, ophicarbonates and soapstone-listwanite. Partial serpentinite is typically grey, preserves obvious primary textures, and contains ca. 30-70 vol% relict minerals (olivine and pyroxenes). In contrast, pervasive serpentinite is light to dark green, contains ca. 0-30 vol% relict minerals, and commonly displays a foliation. The serpentinization process results in volume increases (up to 40%: Komor et al., 1985) and produces alteration minerals

54

Geological Fieldwork 2019, British Columbia Ministry of Energy, Mines and Petroleum Resources, British Columbia Geological Survey Paper 2020-01

(e.g., olivine + H_2O goes to serpentine group minerals + magnetite + awaruite + brucite; Johannes, 1968; Britten, 2017). Carbonatization results in breakdown of the serpentinization minerals (e.g., brucite + CO_2 goes to magnesite + H_2O; Hansen et al., 2005). Increasing the intensity of CO_2 alteration results in a progressive decrease in the volume of the relict serpentinite enclaves from ophicarbonates to soapstone to complete conversion to listwanite. Chemical reactions that change volume (density) and abundance of magnetite can be used as first-order proxies for the degree and type of alteration (Komor et al., 1985; Toft et al., 1990; Hansen et al., 2005; Cutts et al., in press).

5.1. Serpentinization and protolith variability

In partially serpentinized rocks, the serpentinization textures, alteration minerals, and extent of alteration appear to vary between protoliths. In dunite-rich outcrops, serpentine veins are generally subparallel to dunite dikes or layers, rather than penetrating into the surrounding harzburgite or lherzolite (Fig. 4a). In dunite, serpentine veins crosscut primary olivine grains and these veins are progressively thicker and more abundant with increasing degrees of serpentinization (compare Figs. 3a and 3b). In dunite, the pyroxene, if present, is typically strongly altered to bastite.

In contrast, although harzburgite and lherzolite contain serpentine veins (Fig. 3c), with further alteration serpentine principally occurs in the groundmass after olivine and as bastite alteration of pyroxene (Figs. 3d, e). With increasing degree of alteration, bastite colour ranges from beige to dark brown to grey or light yellow, and grain shapes range from subhedral to anhedral (Figs. 3c-e). Altered bastite grains commonly contain secondary magnetite and crosscutting serpentine veins. In partial and pervasive serpentinites, olivine is the least preserved, followed by orthopyroxene and then clinopyroxene (Fig. 3d). Orthopyroxene grains or their bastite equivalents are consistently more altered than clinopyroxene, which typically retains a subhedral shape and high birefringence (Fig. 3e). Olivine-poor pyroxenite-rich dikes are relatively unaltered and the few observed olivine grains, which are interlocked with pyroxene, appear to be the most altered minerals in the assemblage.

5.2. Serpentinite and serpentine texture

Typically, the fresh surface of serpentinite is light to dark grey-green, rarely vibrant green and weathers grey-brown-green to off-white. Pervasive serpentinites locally contain lenses of relatively competent serpentinite in an anastomosing scaly serpentinite matrix and contain serpentine veins parallel to one another (Fig. 4b). Locally, pervasive serpentinites are brecciated, whereas others display polygonal patterns of uniformly spaced serpentine veins (Fig. 4c).

The degree of serpentinization is most effectively determined in thin-section by comparing modal abundances of relict primary versus alteration minerals (Fig. 3), identifying alteration minerals, and distinguishing between serpentine textures. In thin section, Decar serpentinites displays mesh (Figs. 3b, e), hourglass, and ribbon textures, which are typical of the lizardite polymorph. Interlocking (Figs. 3d, e; Fig. 4d) and interpenetrating (Fig. 3e) serpentine textures are also present and likely reflect the antigorite polymorph (Wicks and Whittaker, 1977). Many samples contain a mixture of overprinting textures, indicating multi-stage serpentinization. Figure 3f illustrates an example where an interpenetrating texture overprints interlocking texture and serpentine veins. Serpentine veins occur in samples of all protoliths and extents of serpentinization, but they vary in abundance and can be oriented either parallel or oblique to one another. The veins are white-grey-green and weather to grey-white (Fig. 4c), vary in width from <20 μm to >4 cm, and commonly have a massive, wavy, or interlocking texture and rarely, serpentine selvages (Figs. 3; Figs. 4a-d). Serpentine veins wider than 1 cm are commonly fibrous, and likely composed of chrysotile.

In addition to serpentine and relict primary minerals, serpentinites commonly contain the secondary minerals magnetite (Fig. 3f), brucite (Fig. 3b), awaruite, chlorite, talc, and tremolite, and locally, metamorphic olivine and diopside (Britten, 2017; Milidragovic and Grundy, 2019). Brucite is in both partially and pervasively serpentinized rocks, derived from dunite, harzburgite, and lherzolite protoliths. Brucite most commonly occurs in mesh serpentine or adjacent to relict olivine as discrete grains (<150 μm), aggregates, or as thin veins typically spatially associated with serpentine and/or magnetite (Fig. 3b). In partially serpentinized samples from all protoliths, fine- to coarse- grained magnetite, sulphides, and awaruite are commonly in or close to serpentine veins, whereas in highly serpentinized samples, these minerals are typically in the serpentine groundmass and/or metamorphic olivine. Awaruite grains vary in size (<10 to 800 μm across), shape, and association; they occur as monomineralic grains, locally rimmed by secondary magnetite, or as polymineralic grains intergrown with magnetite and sulphides (e.g., pentlandite, heazlewoodite; Britten, 2017; Milidragovic and Grundy, 2019). Chlorite and talc are common in pyroxene-rich rocks.

6. Carbonate alteration and listwanite

The degree of carbonate alteration and dehydration of ultramafic rocks is highly variable. The CO_2-bearing assemblages form a spectrum consisting of serpentine-magnesite (ophicarbonate), talc-magnesite (soapstone), and quartz-magnesite±fuchsite (listwanite), in order of increasing carbonation. The colour of the rocks, their magnetic susceptibility, and specific gravity vary by the extent to which they have been carbonated (Figs. 4d-f; Cutts et al., in press).

Ophicarbonates are common throughout the Decar area and are nearly indistinguishable from serpentinites in the field but can be identified in thin section and by bulk chemistry. Carbonate minerals occur in partially to highly serpentinized samples or even in samples containing metamorphic olivine. Carbonate veins overprint serpentine veins (±magnetite) and serpentine in groundmass (Fig. 4d), indicating that carbonate

55

Geological Fieldwork 2019, British Columbia Ministry of Energy, Mines and Petroleum Resources, British Columbia Geological Survey Paper 2020-01

alteration post-dated serpentinization. In moderately carbonate-altered samples (Fig. 4e), relict serpentine typically exhibits an interlocking or interpenetrating texture, likely antigorite. Brucite grains occur in weakly carbonated samples but are absent in more carbonated samples. Awaruite, sulphides, and spinel persist except in the most strongly carbonated rocks. In fully carbonated rocks, relict serpentinite is rare, although locally it may occur in small patches, both with or without spinel. Fuchsite is most abundant adjacent to <10 cm thick quartz veins and diminishes in abundance away from the veins (Fig. 4f).

7. Timing of serpentinization and carbonate alteration with respect to dikes in the Trembleur ultramafite

Several generations of non-ultramafic dikes occur in the Decar area. In the Baptiste area, at least some serpentinization and carbonation was after emplacement of a dike that is altered to a rodingite (a non-ultramafic rock that is altered by reduced and alkaline fluids during serpentinization; Barnes et al., 1972; Bach and Klein, 2009; Britten, 2017) and an altered dike of probable Rubyrock igneous complex affinity. A third, relatively fresh fine-grained intermediate dike apparently post-dates serpentinization and is likely Eocene.

8. Discussion and implications
8.1. Origin of dunite

The origin of peridotites in the Trembleur ultramafite has been discussed by Britten (2017), Milidragovic and Grundy (2019) and Grundy (2018). The predominantly harzburgitic mineralogy, with subordinate depleted lherzolite, is consistent with a refractory origin for the Decar peridotites resulting from high degrees of partial melting of a fertile precursor (Britten, 2017; Milidragovic and Grundy, 2019). The harzburgite (±lherzolite) is more depleted (≤2 wt.% Al_2O_3), than the moderately depleted lherzolitic upper mantle (DMM1; 2.38 wt.% Al_2O_3 and ca. 8% clinopyroxene at 1 GPa: Workman and Hart, 2005). Below we consider the origin of the dunite.

Based on fieldwork, the dunite comprises ~15% of the total ultramafic rocks. In contrast, using drill core from the Baptiste deposit, Britten (2017) estimated that dunite makes up only ca. 5% (407 out of 7739 splits) of the peridotite volume at Decar. Britten (2017) may have underestimated the true abundance of dunite because the drill core from Baptiste is highly serpentinized and data were at times collected from splits greater than 5 m. Dunite observed in the field is typically restricted to <0.5 m thick dikes or layers. Consequently, these small dunite bodies could be diluted and misidentified as olivine-rich harzburgite in examination of drill core bulk chemical data (Britten, 2017).

Three origins of dunite have been proposed: 1) as residue from extensive partial melting of fertile peridotite in the mantle (melt fraction >35%; e.g., Takahashi et al., 1993); 2) as a cumulate due to fractionation of olivine from mafic melt or liquids; 3) as a replacement of pyroxene-rich harzburgite or lherzolite by a magnesian±Cr rich magma, commonly at mantle-

crust transition zones in ophiolites (Quick, 1981; Nicolas and Prinzhofer, 1983; Kelemen, 1990). At some localities, multiple origins of dunite have been suggested (e.g., the Trinity peridotite; Quick, 1981), but more commonly, one process is predominant. The relationship of the dunite shape, size, and contacts with the host rock (sharp or diffuse) is important in understanding the origin of dunite (Kelemen, 1990; Kubo, 2002; Morgan and Liang, 2003). However, if highly strained the shape of a dunite body (e.g., lenticular lenses) may no longer reflect the original magmatic process (Nicolas and Prinzhofer, 1983). Residue dunite is best distinguished from other origins by bulk-rock and olivine compositions (Kelemen, 1990; Su et al., 2016). Cumulate dunite typically shows systematic layering, with dunite and chromitite at the base, and troctolitic and/or wehrlite, pyroxenite, and gabbro at the top (Nicolas and Prinzhofer, 1983). Replacement dunite is typically irregularly shaped and displays evidence of volume increase, it may contain traces of clinopyroxene (Kelemen, 1990), and spinel should show a more equant habit relative to that in host rocks (Nicolas and Prinzhofer, 1983; Arai, 1994; Dandar et al., 2019).

The discordant and irregular shaped dunite layers and pods described above resemble replacement dunites described by Kelemen and Ghiorso (1986) and Kelemen (1990). Field and thin section observations suggest that spinel is equant and more abundant in dunite compared to the mostly irregular, vermicular, and commonly fine-grained primary spinel in the surrounding harzburgite. A replacement dunite mechanism would also be consistent with the fine-grained clinopyroxene found in dunite resulting from the consumption of orthopyroxene (Kelemen, 1990). These observations suggest that the dunite at Decar, or at least at Mt. Sidney Williams and the unnamed ridge, may have formed by replacement. Further geochemical characterization is underway to determine the origin of dunite at this locality.

8.2. Serpentinization processes

Field and petrographic observations can place constraints on the timing of serpentinization and the source of hydrothermal fluids. Thin-section and outcrop-scale observations indicate that fluid infiltration during serpentinization of dunite differs from that of harzburgite and lherzolite. Movement of H_2O-rich fluids through dunite was apparently along fractures related to veins compared to less focussed flow in harzburgite and lherzolite (Figs. 3a-d). The grain size and modal abundance of primary minerals (i.e., olivine, pyroxenes, spinel) along with the chemistry and pH of fluids can play an important role in the serpentinization rate and variability (Barnes et al., 1972; Lafay et al., 2012). The overall rate of serpentinization is typically fastest for olivine and slowest for clinopyroxene (Coleman and Keith, 1970; Moody, 1976; Wicks and Whittaker, 1977; Komor et al., 1985); however, this general rule can vary as a function of the composition of the serpentinizing fluid. Olivine may be more resistant to serpentinization than orthopyroxene during interactions with high Mg^{2+}-rich fluids such as during seawater-peridotite interaction. In contrast, orthopyroxene tends to be more resistant than olivine during interactions with fluids that

56

Geological Fieldwork 2019, British Columbia Ministry of Energy, Mines and Petroleum Resources, British Columbia Geological Survey Paper 2020-01

are Si(OH)$_4$-rich; such fluids are generated when seawater reacts with crustal rocks before reaching peridotite (Peacock, 1987; O'Hanley, 1996). Observations of partially serpentinized harzburgite and lherzolite show that olivine grains are the most altered, followed by orthopyroxene; clinopyroxene is relatively unaltered (Fig. 3e). The extent of alteration of these primary minerals could indicate that most of the serpentinization did not occur at the seafloor, which is consistent with isotope data indicating a meteoric fluid source (Britten, 2017).

Protolith composition can exert a primary control on alteration mineral assemblages, along with fluid composition, temperature, and pressure. For example, temperature, oxidation of Fe or high SiO$_2$ can favour formation of serpentine or talc instead of brucite (O'Hanley, 1996; Evans et al., 2013; Sciortino et al., 2015). Harzburgite seems to have a more extensive formation of secondary magnetite relative to dunite which can also be seen in a general higher magnetic susceptibility (Toft et al., 1990; Cutts et al., in press). Possible olivine compositional differences in dunite versus harzburgite could be the cause of variability in awaruite grain size or/and abundance. Future work will explore the formation and stability controls of brucite and awaruite in more detail.

9. Summary

The protoliths of altered rocks in the Trembleur ultramafite are heterogeneous and dunite appears to be more abundant than previously thought. Most of the Trembleur ultramafite is partially to pervasively serpentinized and the primary olivine-pyroxene ratio of the protoliths seems to have exerted a primary control on the types and abundances of alteration minerals, such as brucite and awaruite, and the style of infiltration of serpentinizing fluids. Carbonate alteration post-dated serpentinization, and consumed brucite and awaruite. The heterogeneity in the Trembleur ultramafite protolith and the distribution and extent of alteration thus has implications for the abundance and distribution of brucite and awaruite and therefore on the carbon sequestration and nickel potential of the area.

References cited

Arai, S., 1994. Characterization of spinel peridotites by olivine-spinel compositional relationships: Review and interpretation. Chemical Geology, 113, 191-204.

Bach, W., and Klein, F., 2009. The petrology of seafloor rodingites: Insights from geochemical reaction path modeling. Lithos, 112, 103-117.

Barnes, I., Rapp, J.B., O'Neil, J.R., Sheppard, R.A., and Gude, A.J., 1972. Metamorphic assemblages and the direction of flow of metamorphic fluids in four instances of serpentinization. Contributions to Mineralogy and Petrology, 35, 263-276.

Britten, R., 2017. Regional metallogeny and genesis of a new deposit type - disseminated awaruite (Ni$_3$Fe) mineralization hosted in the Cache Creek terrane. Economic Geology, 112, 517-550.

Coleman, R.G., and Keith, T.E., 1970. A chemical study of serpentinization - Burro Mountain, California. Journal of Petrology, 12, 311-28.

Cordey, F., Gordey, S.P., and Orchard, M.J., 1991. New biostratigraphic data from the northern Cache Creek terrane, Teslin map area, southern Yukon. In: Current Research part E. Geological Survey of Canada, Paper 1991-E, pp. 67-76.

Cutts, J.A., Dipple, G.M., Hart, C., and Milidragovic, D., in press. Assessment of the carbon mineralization potential of British Columbia by quantifying the response of physical properties to the alteration of ultramafic rocks. In: Geoscience BC Summary of Activities 2019: Minerals and Mining, Geoscience BC Report 2020-1.

Dandar, O., Okamoto, A., Uno, M., Oyanagi, R., Nagaya, T., Burenjargai, U., Miyamoto, T., and Tsuchiya, N., 2019. Formation of secondary olivine after orthopyroxene during hydration of mantle wedge: evidence from the Khantaishir Ophiolite, western Mongolia. Contributions to Mineralogy and Petrology, 174, 86.

Eckstrand, O.R., 1975. The Dumont serpentinite: A model for control of nickeliferous opaque mineral assemblages by alteration reactions in ultramafic rocks. Economic Geology, 70, 183-201.

Evans, K.A., Powell, R., and Frost, B.R., 2013. Using equilibrium thermodynamics in the study of metasomatic alteration, illustrated by an application to serpentinites. Lithos, 168/169, 67-84.

Golding, M.L., Orchard, M.J., and Zagorevski, A., 2016. Microfossils from the Cache Creek complex in northern British Columbia and southern Yukon. Geological Survey of Canada, Open File 8033, 25 p.

Grundy, R., 2018. Melting and cooling histories of two upper mantle massifs in the Cache Creek terrane, Central British Columbia. Unpublished B.Sc. Thesis, University of Victoria, Victoria, Canada, 60 p.

Hall, C., and Zhao, R., 1995. Listvenite and related rock-perspectives on terminology and mineralogy with reference to an occurrence at Cregganbaun. Mineralium Deposita, 30, 303-313.

Hansen, L.D., Dipple, G.M., Gordon, T.M., and Kellett, D.A., 2005. Carbonated serpentinite (listwanite) at Atlin, British Columbia: A geological analogue to carbon dioxide sequestration. The Canadian Mineralogist, 43, 225-239.

Johannes, W., 1968. Experimental investigation of the reaction forsterite + H$_2$0 ~ = serpentine + brucite. Contributions to Mineralogy and Petrology, 19, 309-315.

Kelemen, P.B., 1990. Reaction between ultramafic rock and fractionating basaltic magma I. Phase relations, the origin of calc-alkaline magma series, and the formation of discordant dunite. Journal of Petrology, 31, 51-98.

Kelemen, P.B., and Ghiorso, M.S., 1986. Assimilation of peridotite in zoned calc-alkaline plutonic complexes: evidence from the Big Jim complex, Washington Cascades. Contributions to Mineralogy and Petrology, 94, 12-28.

Komor, S.C., Elthon, D., and Casey, J.F., 1985. Serpentinization of cumulate ultramafic rocks from the North Arm Mountain massif of the Bay of Islands ophiolite. Geochimica et Cosmochimica Acta, 49, 2331-2338.

Kubo, K., 2002. Dunite formation processes in highly depleted peridotite: Case study of the Iwanaidake Peridotite, Hokkaido, Japan. Journal of Petrology, 43, 423-448.

57

Geological Fieldwork 2019, British Columbia Ministry of Energy, Mines and Petroleum Resources, British Columbia Geological Survey Paper 2020-01

Lafay, R., Montes-Hernandez, G., Janots, E., Chiriac, R., Findling, N., and Toche, F., 2012. Mineral replacement rate of olivine by chrysotile and brucite under high alkaline conditions. Journal of Crystal Growth, 347, 62-72.

Mihalynuk, M.G., Nelson, J., and Diakow, L J., 1994. Cache Creek terrane entrapment: Oroclinal paradox within Cordillera. Tectonics, 13, 575-595.

Mihalynuk, M.G., Erdmer, P., Cordey, F., Archibald, D.A., Friedman, R.M., and Johannson, G.G., 2004. Coherent French Range blueschist: Subduction to exhumation in less than 2.5 m.y.? Geological Society of America Bulletin, 116, 910-922.

Milidragovic, D., 2019. Geology of the Cache Creek terrane north of Trembleur Lake. British Columbia Ministry of Energy, Mines, and Petroleum Resources, British Columbia Geological Survey Open File 2019-06, 1:50,000 scale.

Milidragovic, D., and Grundy, R., 2019. Geochemistry and petrology of rocks in the Decar area, central British Columbia: Petrologically constrained subdivision of the Cache Creek complex. In: Geological Fieldwork 2018, British Columbia Ministry of Energy, Mines and Petroleum Resources, British Columbia Geological Survey Paper 2019-1, pp. 55-77.

Milidragovic, D., Grundy, R., and Schiarizza, P., 2018. Geology of the Decar area north of Trembleur Lake, NTS 93K/14. In: Geological Fieldwork 2017, British Columbia Ministry of Energy, Mines and Petroleum Resources, British Columbia Geological Survey Paper 2018-1, pp. 129-142.

Monger, J.W.H., and Gibson, H.D., 2019. Mesozoic-Cenozoic deformation in the Canadian Cordillera: The record of a "Continental Bulldozer " ? Tectonophysics, 757, 153-169.

Moody, J.B., 1976. Serpentinization: a review. Lithos, 9, 125-138..

Morgan, Z., and Liang, Y., 2003. An experimental and numerical study of the kinetics of harzburgite reactive dissolution with applications to dunite dike formation. Earth and Planetary Science Letters, 214, 59-74.

Nicolas, A., and Prinzhofer, A., 1983. Cumulative or residual origin for the transition zone in ophiolites: Structural evidence. Journal of Petrology, 24, 2, 188-206.

O'Hanley, D.S., 1996. Serpentinites record of tectonic and petrological history. Oxford University Press, New York, 247 p.

Peacock, S.M., 1987. Serpentinization and infiltration metasomatism in the Trinity peridotite, Klamath province, northern California: Implications for subduction zones. Contributions to Mineralogy and Petrology, 95, 55-70.

Power, I.M., Wilson, S.A., and Dipple, G.M., 2013. Serpentinite carbonation for CO_2 sequestration. Elements, 9, 115-122.

Quick, J.E., 1981. The origin and significance of large, tabular dunite bodies in the Trinity Peridotite, northern California. Contributions to Mineralogy and Petrology, 78, 413-422.

Su, B., Chen, Y., Guo, S., and Liu, J., 2016. Origins of orogenic dunites: Petrology, geochemistry, and implications. Gondwana Research, 29, 41-59.

Schiarizza, P., and MacIntyre, D.G., 1999. Geology of the Babine Lake-Takla Lake area, central British Columbia (93K/11, 12, 13, 14;93N/3, 4, 5, 6). In: Geological Fieldwork 1998, British Columbia Ministry of Energy, Mines and Petroleum Resources, British Columbia Geological Survey Paper 1999-1, pp. 33-68.

Schiarizza, P., and Massey, N.W.D., 2010. Geochemistry of volcanic and plutonic rocks of the Sitlika assemblage, Takla Lake area, central British Columbia (NTS 093N/04, 05, 12, 13). In: Geological Fieldwork 2009, British Columbia Ministry of Energy, Mines and Petroleum Resources, British Columbia Geological Survey Paper 2010-1, pp. 55-67.

Sciortino, M., Mungall, J.E., and Muinonen, J., 2015. Generation of high-Ni sulfide and alloy phases during serpentinization of dunite in the Dumont sill, Quebec. Economic Geology, 110, 733-761.

Struik, L.C., Schiarizza, P., Orchard, M.J., Cordey, F., Sano, H., MacIntyre, D.G., Lapierre, H., and Tardy, M., 2001. Imbricate architecture of the upper Paleozoic to Jurassic oceanic Cache Creek Terrane, central British Columbia. Canadian Journal of Earth Sciences, 38, 495.

Takahashi, E., Shimazaki, T., Tsuzaki, Y., and Yoshida, H., 1993. Melting study of a peridotite KLB-1 to 6.5 GPa, and the origin of basaltic magmas: Philosophical Transactions, Physical Sciences and Engineering, 342, 105-120.

Toft, P.B., Arkani-Hamed, J., and Haggerty, S.E., 1990. The effects of serpentinization on density and magnetic susceptibility: a petrophysical model. Physics of the Earth and Planetary Interiors, 65, 137-157.

Vanderzee, S.S.S., Dipple, G.M., and Bradshaw, P.M.D., 2019. Targeting highly reactive labile magnesium in ultramafic tailings for greenhouse-gas offsets and potential tailings stabilization at the Baptiste deposit, central British Columbia (NTS 093K/13, 14). In: Geoscience BC Summary of Activities 2018: Minerals and Mining, Geoscience BC Report 2019-1, pp. 109-118.

Wicks, F.J., and Whittaker, E.J.W., 1977. Serpentine textures and serpentinization: The Canadian Mineralogist, 15, 459-488.

Workman, R.K., and Hart, S.R., 2005. Major and trace element composition of the depleted MORB mantle (DMM). Earth and Planetary Science Letters, 231, 53-72.